

Cylindrical shear resistance of helical piles subjected to seismic loads

Gustavo Padros
ARKK Engineering Corp., Sherwood Park, Alberta, Canada
Richard Schmidt
Almita Piling Inc., Edmonton, Alberta, Canada



ABSTRACT

The design of helical piles in seismic regions should consider the detrimental effects produced by dilatational and shear waves travelling through soils. The dilatational wave produces an increase in pore pressure, which leads to a decrease in the effective stress and consequently a decrease in the soil shear strength. Furthermore, dynamic shear stresses are produced due to the propagation of shear waves and due to the increase in pile loads caused by the overturning moment acting on the superstructure.

Helical piles manufactured with multiple helices derive their compressive resistance from shaft friction, cylindrical shear resistance (CSR) and end bearing. Given that the displacement to fully mobilize end bearing is relatively large, helical piles subjected to seismic loading must rely on cylindrical shear to resist the increment in compressive load if large settlements are to be avoided. A methodology based on Zeevaert's theory is presented in the present paper that allows designing CSR for seismic loads.

RÉSUMÉ

La conception des pieux hélicoïdaux dans les régions sismiques devrait prendre en compte les effets néfastes produits par les ondes de dilatation et de cisaillement se propageant dans les sols. La vague de dilatation produit une augmentation de la pression dans les pores, ce qui entraîne une diminution de la contrainte effective et, par conséquent, une diminution de la résistance au cisaillement du sol. De plus, des contraintes de cisaillement dynamiques sont générées en raison de la propagation des ondes de cisaillement et de l'augmentation des charges de pieu causées par le moment de renversement agissant sur la superstructure.

Les pieux hélicoïdaux fabriqués avec plusieurs hélices tirent leur résistance à la compression du frottement de l'arbre, de la résistance au cisaillement cylindrique (CSR) et du roulement en bout. Étant donné que le déplacement pour mobiliser complètement le palier d'extrémité est relativement important, les pieux hélicoïdaux soumis à une charge sismique doivent s'appuyer sur un cisaillement cylindrique pour résister à l'augmentation de la charge de compression si l'on veut éviter des dépôts importants. Le présent article présente une méthodologie basée sur la théorie de Zeevaert qui permet de concevoir la CSR pour les charges sismiques.

1 INTRODUCTION

Dilatational waves and shear waves are generated when the seismic waves produced by earthquakes reach the firm ground / soils deposits interphase. The dilatational waves travel faster than the shear waves and are the first to arrive at the place of observation. The translation of dilatational waves requires changes in the soil volume. Therefore, in saturated soils they produce high pore water pressures although small displacements. On the contrary, shear waves do not produce volume changes in the soil during their propagation, but high shear distortions may be induced and shear stresses greater than the soil shear strength can be developed.

Dilatational waves and shear waves are important for the design of deep foundations. The surface (Rayleigh) wave is a third type of seismic wave, developed once the other waves reach the surface and is not considered herein.

Helical piles may develop considerable compressive and uplift resistances, which make them viable as a

deep foundation alternative in earthquake regions. The pile compressive resistance comprises shaft friction and end bearing, and if the helical pile has been manufactured with several helices installed relatively close (typically spaced apart not more than 3 times the helix diameter), a cylindrical shear resistance (CSR) is developed between the uppermost and lowermost helices, which also contributes to the compressive resistance of the pile. Furthermore, the uplift resistance of the helical pile comprises shaft friction and upward bearing of the uppermost helix. Piles manufactured with multiple helices adequately spaced also develop cylindrical shear resistance in uplift loading.

The Canadian Foundation Engineering Manual (CFEM, 2006) includes design equations to compute the compressive and uplift resistance of helical piles applying Limit States Design (LSD), Ultimate Limit States (ULS) and Service Limit States (SLS). Once the soil shear strength parameters have been accurately determined, including the effects of soil disturbance, the equations provide adequate results. However, in the case of earthquake conditions, additional soil shear

stresses have to be considered due to the presence of seismic shear waves and due to the increase in pile loads caused by the overturning moment acting on the superstructure. Furthermore, the dilatational wave produces an increase in pore pressure, which leads to a decrease in the effective stress and consequently a decrease in the soil shear strength. On this basis, the design of helical piles in earthquake regions requires analyzing the combined effects of an increase in soil shear stress (due to shear wave action plus greater pile loads due to the structure overturning moment) and a decrease in soil shear strength (due to an increase in pore pressure).

A well designed helical pile subjected to compressive load will develop a relatively small vertical displacement when loaded to service conditions, typically less than 6 mm. At this load level and vertical displacement, the pile may have developed full mobilization of shaft friction, partial mobilization of CSR and small mobilization of end bearing. Given that the displacement to fully mobilize end bearing is relatively large and that no more shaft friction is available, helical piles subjected to seismic loading must rely on cylindrical shear to resist the increment in compressive load if large settlements want to be avoided. Understanding of CSR thus becomes of great importance in the design of helical piles subjected to seismic loading.

The objectives of the present paper are: (1) Discuss the influence of the dilatational and seismic waves on the CSR of helical piles; (2) Apply Zeevaert's theory (1980, 1982, 1988, 1991) to determine the decrease in soil shear strength and the increase in the soil shear stress due to earthquakes; and (3) Compute the CSR developed when seismic loads are present.

2 GENERAL INFORMATION ON HELICAL PILES

A helical pile consists of one or more helix-shaped steel plates welded to a steel pipe. The components of a helical pile are illustrated in Figure 1, where a double helix pile is depicted. Helical piles are installed by applying torque at the pile head, forcing the pile to rotate. Penetration into the soil is achieved due to the helical shape of the steel plates.

The helix spacing is expressed in terms of the helix diameter. Typical helix spacing ranges from 2 to 3 times the helix diameter. Once a helix spacing has been proposed, the exact helix spacing is chosen as a multiple of the pitch (i.e, the vertical distance between the upper and lower ends of a helix), such that in ideal pile installation conditions the penetration path of the lowermost helix will be followed by the rest of the helices, minimizing soil disturbance.

A helix spacing up to about 3 times the helix diameter allows for cylindrical shear resistance (CSR) to develop, which considers the development of a cylindrical shaped failure plane, extending vertically between the helices (as shown in Figure 2). The CSR contributes to the compressive and uplift resistance of the pile. The use of direct shear test results to

understand the development of CSR under static loading has been applied by Padros (2013-1 and -2).

Helical piles are typically installed open-ended. The pile tip is cut at a 45 degree angle to facilitate penetration into the soil. As the pile penetration proceeds, the tip will eventually become plugged with soil. End bearing computations typically consider an area comprising the exterior footprint of the lowermost helix, meaning that plugged tip conditions are considered.

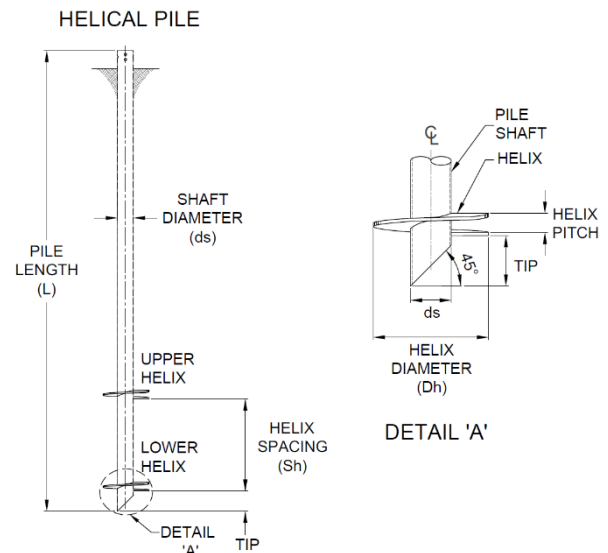


Figure 1. Components of a helical pile

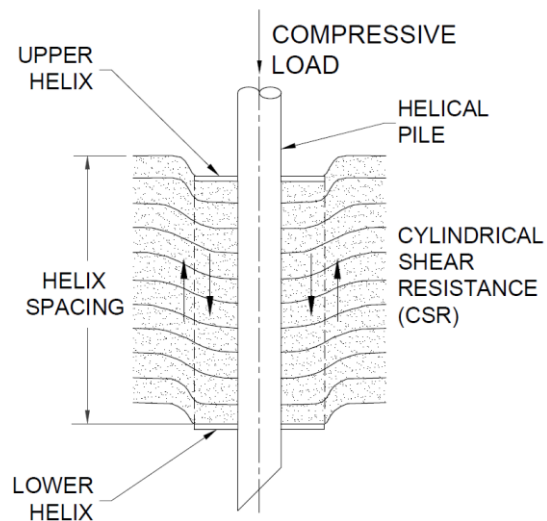


Figure 2. Cylindrical shear resistance (CSR).

Equations to compute the compressive and uplift resistances of helical piles can be found in the CFEM (2006). The pile compressive resistance comprises shaft friction and end bearing. The uplift resistance of

the helical pile comprises shaft friction and upward bearing of the uppermost helix, unless this is too shallow. If the piles have multiple helices not spaced more than 3 times the helix diameter, then CSR will develop, and will contribute to both compressive and uplift resistances.

3 INCREMENT IN PORE WATER PRESSURE DUE TO DILATATIONAL WAVE

The increment in pore water pressure due to dilatational waves has been studied by Zeevaert (1991), who developed a methodology based on the following rationale:

- (a) The dilatational wave propagates from firm ground to the surface according to the following equation:

$$v_d^2 \frac{\delta^2 w}{\delta z^2} = \frac{\delta^2 w}{\delta t^2} \quad [1]$$

where w is the vertical displacement and v_d is the dilatational wave velocity

- (b) From theory of elasticity we know that the soil pressure σ_z is given by:

$$\sigma_z = E_c \frac{\delta w}{\delta z} \quad [2]$$

where E_c is the dynamic soil modulus, given by :

$$E_c = 2(1 + \nu)\mu \quad [3]$$

where ν is the Poisson ratio and μ is the shear modulus, equal to :

$$\mu = v_d^2 \rho \frac{(1-2\nu)}{2(1-\nu)} \quad [4]$$

where ρ is the unit mass of the soil, equal to the soil unit weight γ divided by the gravitational acceleration.

- (c) Zeevaert (1991) solves Equation 2 as:

$$\sigma_z = -E_c w_o \frac{\pi}{2D} \sin\left(\frac{\pi z}{2D}\right) \quad [5]$$

where w_o is the vertical displacement amplitude, given by :

$$w_o = \frac{4D^2}{\pi^2} \frac{\rho}{E_c} G_{av} \quad [6]$$

where G_{av} is the maximum vertical ground surface acceleration.

- (d) Substituting Equations 3, 4 and 6 in 5 we obtain:

$$\sigma_z = -\left(\frac{2}{\pi} G_{av} D \rho\right) \sin\left(\frac{\pi z}{2D}\right) \quad [7]$$

- (e) Considering that during the earthquake, the increase in soil pressure in the saturated soil sediment occurs at constant volume, requiring the decrease in soil effective stress to be equal to increase in pore water pressure, $\sigma_z = -u_z$, hence:

$$u_z = \left(\frac{2}{\pi} G_{av} D \rho\right) \sin\left(\frac{\pi z}{2D}\right) \quad [8]$$

Equation 8 can be used to determine the increment in pore water pressure caused by the dilatational shear wave.

4 INCREMENT IN SOIL SHEAR STRESS DUE TO SHEAR WAVE

The shear waves propagate from the firm ground interphase into the soil deposits, producing important shear distortions in the soil mass. These distortions cause an increase in shear stress which is additive to the static shear stress acting on the soil prior to the earthquake (Figures 3 and 4). Furthermore, the shear waves are slower than the dilatational waves and hence arrive later at the place of observation. On this basis, it is considered that the pore pressure caused by the dilatational wave has already increased by the time the shear waves arrive at the foundation.

The increment in soil shear stress due to shear waves has been studied by Zeevaert (1980, 1982, 1988 and 1991), who presented the following methodology for the computation of the shear stress:

- (a) The time required by the shear wave to travel through the full soil deposit, from firm ground to the surface, is equal to $\frac{1}{4}$ the soil dominant period T , therefore:

$$\frac{1}{4}T = \frac{D}{v_s} \quad [9]$$

where D is the depth between the ground surface and the firm ground, and v_s is the shear wave velocity. In stratified soil deposits, Equation 9 is modified as follows:

$$\frac{1}{4}T = \sum_{i=1}^n \frac{d_i}{(v_s)_i} \quad [10]$$

- (b) The shear wave velocity is a function of the dynamic shear modulus μ as follows :

$$v_s^2 = \frac{\mu}{\rho} \quad [11]$$

- (c) The dynamic shear modulus μ can be determined in the field from seismic cone penetration tests, crosshole seismic surveys, downhole seismic surveys, or other field tests. Alternatively, it may be determined through laboratory tests in soil samples, which may include resonant column tests, free torsion pendulum tests or other.
- (d) The shear wave propagates from firm ground to the surface according to the following equation:

$$v_s^2 \frac{\delta^2 u}{\delta z^2} = \frac{\delta^2 u}{\delta t^2} \quad [12]$$

where u is the vertical displacement. Since the values of μ , ρ and consequently v_s change for every soil layer, Zeevaert (1982), developed an integration method to solve Equation 12 as follows:

- (e) The algorithms for the computation of the maximum horizontal displacements δ_i and the corresponding shear stresses τ_i in each soil layer for the ground motion induced by the shear waves are given by:

$$\delta_{i+1} = A_i \delta_i - B_i \tau_i \quad [13]$$

$$\tau_{i+1} = C_i (\delta_i + \delta_{i+1}) + \tau_i \quad [14]$$

where the coefficients have the following values :

$$A_i = \frac{1 - N_i}{1 + N_i} \quad [15]$$

$$B_i = \frac{1}{1 + N_i} \left(\frac{\delta_i}{\mu_i} \right) \quad [16]$$

$$C_i = \frac{1}{2} \rho \delta_i \omega_n^2 \quad [17]$$

$$N_i = \frac{\rho \delta_i^2 \omega_n^2}{4\mu_i} \quad [18]$$

and ω_n is the angular frequency of the soil mass, which initially can be computed from the soil period as follows:

$$\omega_n = \frac{2\pi}{T} \quad [19]$$

- (f) The calculations start by computing a ground surface displacement δ_1 equal to :

$$\delta_1 = \frac{G_{av}}{\omega_n} \quad [20]$$

and assume that the increment in shear stress at the ground surface due to the shear wave is zero ($\tau_1 = 0$).

- (g) Subsequently Equations 13 and 14 are computed for each soil layer starting from the ground surface, using the coefficients in equations 15 to 18.
- (h) When the calculations reach firm ground, the horizontal displacement computed should be zero. If this is not the case, the angular frequency initially assumed in Equation 19 should be corrected and a new iteration undertaken from the ground surface to the firm ground.

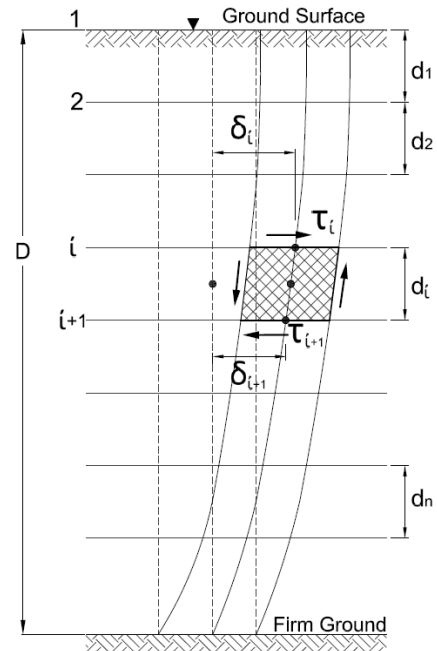


Figure 3. Shear stress due to shear wave.

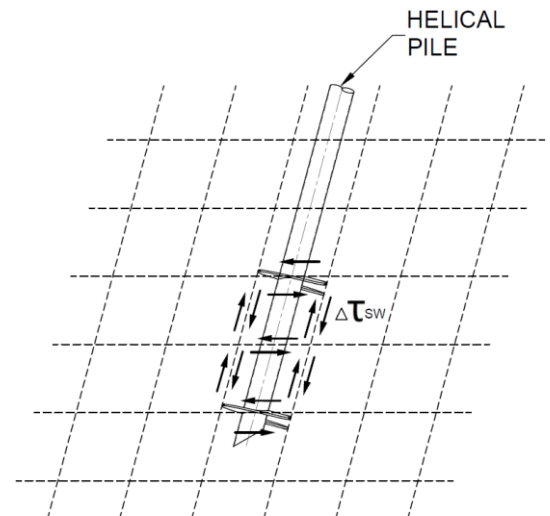


Figure 4. Shear stress on helical pile CSR due to shear wave

5 INCREMENT IN SOIL SHEAR STRESS DUE TO OVERTURNING MOMENT TRANSFERRED TO PILES SUPPORTING RIGID STRUCTURES

The present Section considers a rigid superstructure on a rigid mat or box foundation supported by helical piles, as shown in Figure 5. It is assumed that the underside of the foundation slab is not in contact with the soil underneath, therefore the vertical loads acting on the structure are directly transferred to the helical piles.

As the result of an earthquake, a horizontal seismic shear force V_M will be produced on a structure, acting on its centre of mass located on a height h_M , producing a seismic overturning moment O_{TM} as shown in Figure 5. The overturning moment will produce dynamic loads on the piles, which will be additional to the static loads previously acting.

The procedure to determine the horizontal seismic shear force acting on the structure is included in Building Codes. The present Section does not summarize any procedure, rather it is assumed that the overturning moment has already been computed.

The determination of the dynamic loads transferred to the piles requires undertaking soil-structure interaction calculations. For the purposes of the present paper, a simple approach is presented, consisting on computing the increase in pile load ΔP_i due to earthquake using the following equation:

$$\Delta P_i = \frac{M_y x}{\sum x^2} + \frac{M_x y}{\sum y^2} \quad [21]$$

where M_y and M_x the factored overturning moments due to earthquake loading and x and y are the distances of the piles to the center of gravity of the foundation. On this basis, the increase in the shear stress between the helices ΔCSR due to the increase in pile load ΔP_i due to earthquake is:

$$\Delta CSR = \frac{\Delta P_i}{\pi (D_h) (2 D_h)} \quad [22]$$

The pile compressive resistance comprises shaft friction, end bearing and CSR. The latter is applicable to helical piles manufactured with multiple helices spaced not more than 3 times the helix diameter. The vertical displacement of a helical pile subjected to service conditions will typically be sufficient to develop full mobilization of shaft friction, partial mobilization of CSR and small mobilization of end bearing, which requires relatively large displacements to fully develop. On this basis, a conservative assumption is that the CSR alone will have to resist the increase in pile load, which therefore requires the allowance of additional CSR resistance when helical piles in seismic regions are designed.

Once the decrease in soil shear strength and the increase in the soil shear stress due to earthquakes has been determined, the next step is to carry out laboratory tests to find out if the soil has adequate resistance to develop the necessary CSR to support the seismic loads. Triaxial cyclic tests or direct shear tests (cyclic or

conventional) may be carried out. Direct shear tests are particularly desirable since the distortion produced in the soil sample during the test resembles the distortion of the soil between the helices when a helical pile is loaded in the field. The use of direct shear test results to understand the development of CSR under static loading has been applied by Padros (2013-1 and -2).

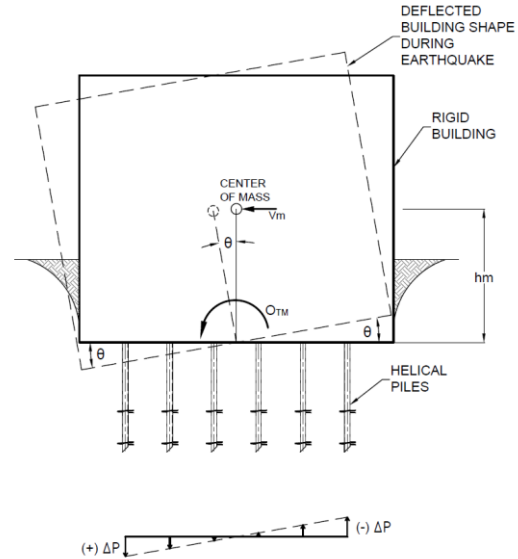


Figure 5. Pile loads due to overturning moment

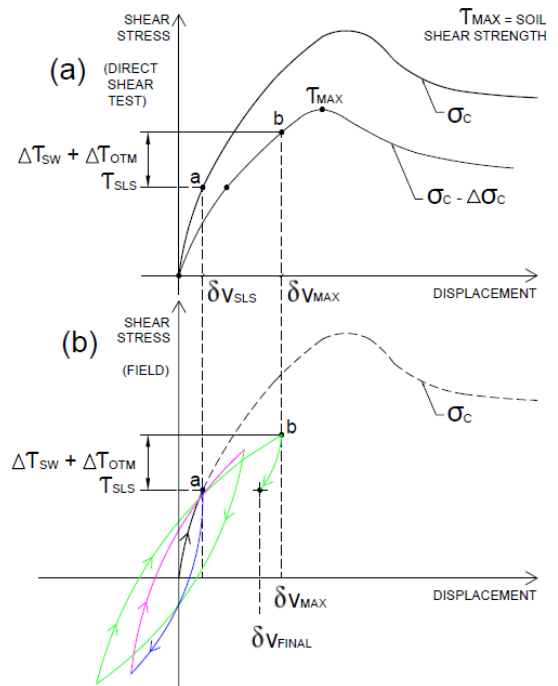


Figure 6. Shear stress increase acting on CSR

On this basis, the methodology presented in Sections 3, 4 and 5 is shown in Figure 6, where $\Delta\tau_{sw}$ is the additional soil shear stress due to the shear waves and $\Delta\tau_{OTM}$ is the additional soil shear stress due to the increase in pile loads caused by the overturning moment acting on the superstructure. The confinement effective stress between the helices is σ_c . Furthermore, the dilatational wave produces an increase in pore pressure, which leads to a decrease in the confinement effective stress $\Delta\sigma_c$. Therefore, the direct shear test is carried out applying a compressive effective stress $\sigma_c - \Delta\sigma_c$. In that test, the total increase in shear stress due to seismic loads is $\Delta\tau_{sw} + \Delta\tau_{OTM}$, which has to be compared with the maximum shear resistance of the soil.

6 EXAMPLE OF CSR COMPUTATION CONSIDERING SEISMIC CONDITIONS

6.1 General

An example is presented to illustrate the computation of the CSR of a helical pile subjected to seismic load. The example considers a rigid superstructure on a rigid shallow foundation supported by helical piles, as shown in Figure 7. The ULS and SLS static compressive loads on each pile are 45 ton and 32 ton, respectively. The overturning moments in the X and Y directions are 1,000 ton-m and 600 ton-m, respectively. A maximum vertical ground surface acceleration G_{av} of 1 m/sec^2 is considered. The subsurface conditions correspond to a stratified deposit comprising granular and cohesive soil layers extending to 24 m depth, where firm ground is encountered. The groundwater level is located at the ground surface. The unit weight γ and the shear strength parameters (undrained shear resistance C_u and angle of internal friction ϕ) of each soil layer are presented in Table 1.

All helical piles have the same size, consisting of a 273 mm shaft diameter and two helices 762 mm diameter, located at 12.24 m and 13.76 m depth (therefore the helix spacing is 1.524 m). The piles head is at 2 m depth and is pinned to the slab. The piles length is 12 m, extending from 2 m to 14 m depth.

Table 1. Soil properties and parameters

Layer	z (m)	Soil Type	γ (ton/m ³)	Vs (m/s)	Cu (ton/m ²)	ϕ (deg)
A	0 – 6	Sand	1.85	90	0	28
B	6 – 10	Clay	1.80	50	15	0
C	10 – 16	Sand	1.90	100	0	30
D	16 – 20	Clay	1.95	70	10	0
E	20 – 24	Sand	2.00	120	0	32

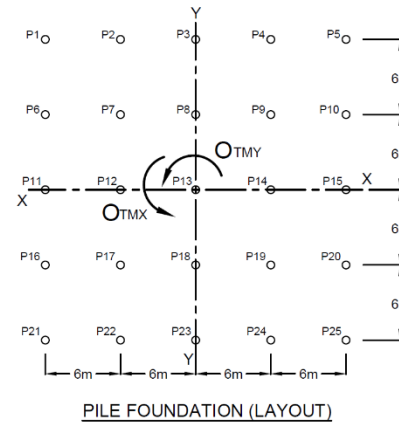
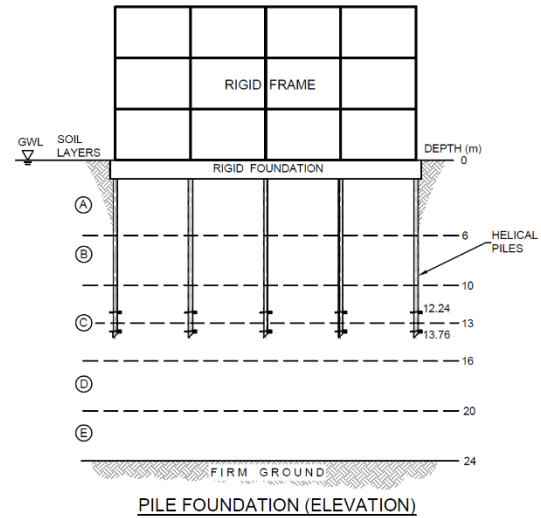


Figure 7. Building and soils conditions used in example

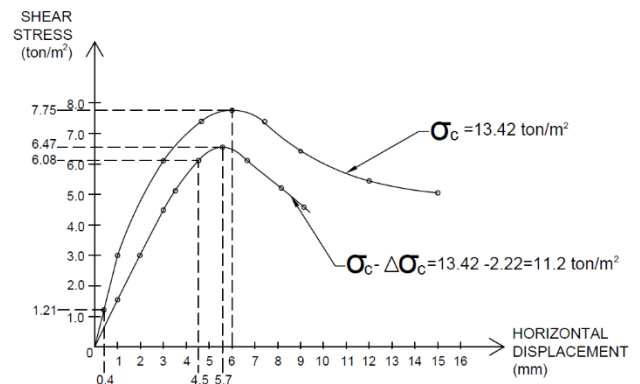


Figure 8. Shear stress computation based on the results of a direct shear test.

The unfactored compressive resistance of the helical pile is 210 ton, comprising a shaft friction of 20 ton, CSR of 30 ton and an end bearing of 160 ton. Based on CFEM, applying a geotechnical resistance factor of 0.4 for deep foundations, the resulting factored geotechnical resistance is 84 ton, adequate to support the ULS compressive load of 45 ton.

6.2 Considerations

The computation of the CSR is based on the following considerations:

- (a) Rigid superstructure on a rigid shallow foundation.
- (b) The vertical loads acting on the structure are directly transferred to the helical piles.
- (c) Shear waves do not produce volume changes or pore pressures in the soil during their propagation. However, the increase in pore pressure produced by the dilatational waves, which arrive first to the deep foundation location, is assumed to be still present once the shear waves arrive.
- (d) The increase in soil shear stress (due to shear wave action and due to greater pile loads caused by the structure overturning moment) occurs at the same time the soil shear strength decreases (due to an increase in pore pressure).
- (e) Soil is saturated.
- (f) The SLS load acting on each pile is 32 ton. Considering that a small vertical pile displacement has developed under service conditions, sufficient to fully mobilize the shaft friction but negligible mobilization of end bearing has occurred, then the CSR mobilized under SLS conditions is about 32 ton – 20 ton = 12 ton. Therefore, the CSR available to resist the increase in load due seismic forces is about 30 ton – 12 ton = 18 ton.
- (g) The vertical effective stress at mid height between the helices (13 m depth) under static conditions is $11 \text{ ton/m}^2 + 4.84 \text{ ton/m}^2 = 15.84 \text{ ton/m}^2$, where 11 ton/m^2 is the vertical stress prior to pile installation and 4.84 ton/m^2 is the increase in vertical stress caused by the loaded pile under static conditions.
- (h) The confining effective stress increases in the proximity of the pile after this has been installed. On this basis, the confining effective stress at mid height between the helices under static conditions is considered equal to about 1.2 times the vertical effective stress (therefore equal to 13.4 ton/m^2).

- (i) The shear stress acting in the soil on vertical planes between the helices under static pile loading conditions was calculated as $(15.84 \text{ ton/m}^2 - 13.4 \text{ ton/m}^2)/2 = 1.21 \text{ ton/m}^2$
- (j) The dynamic shear modulus was determined in the field from seismic cone penetration tests.

6.3 CSR Computation

(a) Initial calculations

The shear modulus and the ratios $\frac{d_i}{(v_s)_i}$ are presented in Table 2. From that Table and Equations 10, 19 and 20 we obtain the soil period $T = 1.2 \text{ sec}$, angular frequency $\omega_n = 5.3 \text{ sec}^{-1}$ and ground surface displacement $\delta_1 = 0.03 \text{ m}$.

Table 2. Soil mass, shear modulus and $d_i/(Vs)_i$ ratios.

Layer	d_i (m)	ρ ($\text{ton} \cdot \text{sec}^2 / \text{m}^4$)	μ (ton/m^2)	$d_i/(Vs)_i$ (sec)
A	6	1.85	1,525	0.067
B	4	1.80	450	0.080
C	6	1.90	1,950	0.060
D	4	1.95	975	0.057
E	4	2.00	2,950	0.033

(b) Increment in pore pressure caused by dilatational wave

The increment in pore water pressure is computed from Equation 8, considering an average unit mass of the soil ρ equal to $0.193 \text{ ton} \cdot \text{sec} / \text{m}^4$. Substituting the parameters in Equation 8, we obtain the increment in pore water pressure caused by the dilatational wave, computed given by the equation below. The results are summarized in Table 3.

$$u_z = \left[\frac{2}{\pi} \left(1 \frac{\text{m}}{\text{sec}^2} \right) 24 \text{ m} \left(0.193 \frac{\text{ton} \cdot \text{sec}^2}{\text{m}^4} \right) \right] \sin \left(\frac{\pi}{2} \frac{z}{24 \text{ m}} \right)$$

$$u_z = 2.95 \sin \left(\frac{\pi z}{48} \right)$$

Table 3. Increment of pore water pressure due to dilatational wave.

z (m)	U_z (ton/m^2)	z (m)	U_z (ton/m^2)	z (m)	U_z (ton/m^2)
0	0	10	1.80	18	2.73
2	0.39	12	2.09	20	2.85
4	0.76	13	2.22	22	2.92
6	1.13	14	2.34	24	2.95
8	1.48	16	2.55		

(c) Increment in soil shear stress due to shear wave

From Equation 20 the ground surface displacement $\delta_1 = 0.03$ m is obtained. In accordance to the method hypothesis, the increment in shear stress at the ground surface due to the shear wave is zero ($\tau_1 = 0$). Subsequently, Equations 13 and 14 are computed for each soil layer starting from the ground surface, using the

coefficients in equations 15 to 18. The results are included in Table 4. The computation results indicate that the horizontal displacement computed at firm ground is zero, which indicates that the angular frequency initially assumed in Equation 19 is correct, and there is no need to carry out another iteration.

Table 4. Computation of increment of soil shear stress and displacements due to shear wave

Depth (m)	Layer	d_i (m)	ρ (ton-sec ² /m ⁴)	μ (ton/m ²)	$N_i \times 10^{-3}$	A_i	$B_i \times 10^{-3}$	C_i (ton/m ³)	δ_i (m)	τ_i (ton/m ²)
0									0.03	0
6	A	6	1.85	1,525	36.2	0.93	3.80	18.42	0.029	1.10
10	B	4	1.80	450	52.9	0.90	8.44	11.89	0.017	1.64
16	C	6	1.90	1,950	7.27	0.99	1.53	9.45	0.011	2.17
20	D	4	1.95	975	25.9	0.95	4.00	12.61	0.002	2.33
24	E	4	2.00	2,950	8.99	0.98	1.34	13.26	0	2.33

(d) Increment In soil shear stress due to overturning moment transferred to piles supporting rigid structures

The increase in pile load ΔP_i due to earthquake is computed using Equation 21, considering $\Sigma x^2 = \Sigma y^2 = 1,800$ m². The maximum increase will occur in the corner piles (designated No's. 1, 5, 21 and 25 in Figure 7), obtaining $\Delta P_i = \pm 10.7$ ton in each of them.

Consequently, the increase in the shear stress between the helices due to the increase in pile load ΔP_i due to earthquake is:

$$\Delta CSR = \frac{\Delta P_i}{\pi (D_h) (2 D_h)} = \frac{10.7 \text{ ton}}{\pi (0.762 \text{ m}) (2 \cdot 0.762 \text{ m})} =$$

$$\Delta CSR = 2.93 \frac{\text{ton}}{\text{m}^2}$$

(e) Computation of CSR increase

As mentioned in consideration (i), the initial shear stress acting on the soil under static conditions (on vertical planes between the helices) was assumed to be 1.21 ton/m². The increase in shear stress due to shear wave action and due to greater pile loads caused by the structure overturning moment should be added to this stress, as follows:

Based on the calculations undertaken in the previous Sections, the total increase in the shear stress in vertical planes between the helices ΔCSR_{TOTAL} is equal to:

$$\Delta CSR_{TOTAL} = 1.94 \frac{\text{ton}}{\text{m}^2} + 2.93 \frac{\text{ton}}{\text{m}^2} = 4.87 \frac{\text{ton}}{\text{m}^2}$$

which produces a cylindrical shear force equal to 17.8 ton, which is basically the CSR that was available to resist the increase in load due seismic forces, as mentioned in consideration (f).

Therefore, the total CSR adding the static plus the dynamic increment is:

$$CSR_{TOTAL} = 1.21 \frac{\text{ton}}{\text{m}^2} + 4.87 \frac{\text{ton}}{\text{m}^2} = 6.08 \frac{\text{ton}}{\text{m}^2}$$

In order to determine the effect that the increase in pore pressure has in the shear resistance, direct shear tests can be carried out in representative soil samples retrieved from the soil layers where the helices will be located. In the present example, the results from direct shear tests undertaken in a sample obtained from the sand layer located at 13 m depth are shown in Figure 8. The figure shows the results of the shear stress and displacement developed applying a compressive stress of 13.4 ton/m². The results of a second test where the increase in pore pressure was deducted from the compressive stress are also shown (i.e., 13.4 ton/m² - 2.2 ton/m² = 11.2 ton/m²). Based on the comparison between the two tests it is noticed that the maximum shear resistance decreases from 7.75 ton/m² to 6.47 ton/m² due to the increase in pore pressure. Furthermore, it is observed that the CSR has adequate resistance to support the total shear stress acting between the helices (i.e., 6.08 ton/m² < 6.47 ton/m²). A rough estimate of the maximum pile vertical displacement produced during the earthquake, additional to the previous pile vertical displacement under service conditions, may be obtained from Figure 8, equal to about 4.5 mm - 0.4 mm = 4.1 mm, which is a conservative estimate because the end bearing was neglected in the pile resistance under earthquake loading. This pile vertical displacement would not be

permanent, but would decrease once the dynamic loading disappears and the increment in pore pressure dissipates.

7 CONCLUSIONS

1. Soil deposits subjected to seismic loading experience an increase in shear stress and a decrease in shear strength. These should be taken into consideration in the design of foundations.
2. Increases in shear stress result from the propagation of seismic shear waves and due to the increase in pile loads caused by the overturning moment acting on the superstructure. Furthermore, the dilatational wave produces an increase in pore pressure, which leads to a decrease in the effective stress and consequently a decrease in the soil shear strength.
3. The increase in shear stress due the shear wave and the decrease in shear strength due to the dilatational wave can be determined applying Zeevaert's theory (1980, 1982, 1988 and 1991). The methodology to determine the increase in pile loads caused by the seismic overturning moment can be found in Building Codes.
4. Helical piles can be designed to have adequate resistance against seismic loads by a proper design of CSR. This requires leaving additional CSR resistance under SLS conditions such that when the earthquake comes, the CSR still has capacity to take the full seismic load. Small pile displacements should be expected, given that small pile vertical displacements are required to develop CSR.
5. Helical piles are a type of deep foundation well suited to support seismic loads when properly designed.

ACKNOWLEDGEMENT

The Authors are grateful to Hector Ibarra, P. Eng. with Almita Piling Inc. for his help preparing the figures.

REFERENCES

- Canadian Geotechnical Society, 2006. *Canadian Foundation Engineering Manual*. Third Edition, Vancouver.
- Padros, G. (2013). Analysis of Cylindrical Shear Resistance of Screw Piles Subjected to Compressive Loads Based on Direct Shear Tests. *1st International Symposium on Helical Piles*. Amherst, Massachusetts.
- Padros G. (2013). Influence of Helix Geometric Configuration on the Cylindrical Shear Resistance of Screw Piles Based on Direct Shear Tests. *Canadian Geotechnical Conference*, Montreal, Quebec.
- Padros, G. and Schmidt, R. (2018). Performance of Helical Pile Cylindrical Shear Resistance in Earthquake Loading. *12th Canadian Conference on Earthquake Engineering*. Quebec, QC.
- Zeevaert, Leonardo (1980). *Interaccion Suelo – Estructura de Cimentacion*. Editorial Limusa. Mexico.
- Zeevaert, Leonardo (1982). *Foundation Engineering for Difficult Subsoil Conditions*. Second Edition. Van Nostrand Reinhold, New York.
- Zeevaert, Leonardo (1988). *Seismo-Geodynamics of the Ground Surface*. Editora e Impresora Internacional, S.A de C.V., Mexico.
- Zeevaert, Leonardo (1991). "Foundation Problems in Earthquake Regions". *Foundation Engineering Handbook*. Fang, H.Y. (Editor). Second Edition. Chapman & Hall, New York.